Cell. Mol. Life Sci. 66 (2009) 1985 – 1997
1420-682X/09/111985-13
DOI 10.1007/s00018-009-9179-2

Cellular and Molecular Life Sciences

Research Article

A nucleic acid-hydrolyzing antibody penetrates into cells via caveolae-mediated endocytosis, localizes in the cytosol and exhibits cytotoxicity

J. Y. Jang[a], J. G. Jeong[a], H. R. Jun[a], S. C. Lee[b], J. S. Kim[c], Y. S. Kim[d, *], and M. H. Kwon[a, *]

[a] Department of Microbiology, Ajou University School of Medicine, Suwon 443 – 721 (Korea), Fax: +82-31-219-5079, e-mail: kwonmh@ajou.ac.kr
[b] Department of Genetic Engineering, Sungkyunkwan University, 300 Chunchun-dong, Jangan-gu, Suwon 440 – 746 (Korea)
[c] Department of Chemistry, College of Natural Science, Chonnam National University, 300, Yongbong-dong, Buk-gu, Gwangju 500 – 757 (Korea)
[d] Department of Molecular Science and Technology, Ajou University, Suwon 443 – 749 (Korea), Fax: +82-31-219-2394, e-mail: kimys@ajou.ac.kr

Received 05 March 2009; accepted 20 March 2009
Online First 14 April 2009

Abstract. Many natural anti-DNA antibodies (Abs) have the ability to translocate across the plasma membrane and localize in the nucleus of mammalian cells, frequently leading to cytotoxicity to cells. Herein, we report detailed intracellular trafficking routes and cytotoxicity in HeLa cells for a single chain variable fragment (scFv) Ab, 3D8, which is an anti-DNA Ab capable of hydrolyzing both DNA and RNA. The intracellular penetration of 3D8 scFv occurred by caveolae/lipid raft endocytosis. The time-course chasing experiments revealed that 3D8 scFv escaped directly from the caveosome into the cytosol and remained in the cytosol without further trafficking into endosomes, lysosomes, endoplasmic reticulum, Golgi, or nucleus. The cytosolically localized 3D8 scFv maintained its nuclease activity to hydrolyze cellular RNAs, mainly mRNAs, eventually triggering apoptotic cell death. Our results demonstrate that 3D8 scFv has a unique intracellular trafficking route of localizing in the cytosol, thereby exhibiting cytotoxicity due to its nuclease activity.

Keywords. Anti-DNA antibody, 3D8 scFv, endocytosis, RNA-hydrolysis, cell death.

Introduction

In addition to their DNA binding and/or hydrolyzing activities, some anti-DNA antibodies (Abs), preferentially found in humans and mice with autoimmune diseases, have been shown to possess the ability to penetrate into living cells, for example the cell penetrating peptides (CPPs) [1, 2]. Unlike CPPs which do not generally exhibit cytotoxicity, cell-penetrating anti-DNA Abs with DNA-hydrolyzing activity induced apoptotic cell death [3, 4]. Even though their cell-penetrating capacity has not yet been investigated in detail, some polyclonal anti-DNA Abs have shown that their DNA-hydrolyzing activity is correlated with cytotoxicity to tumor cells [5, 6].

* Corresponding authors.

Several studies revealed that the internalizing capacity of anti-DNA Abs might be attributed to the antigen binding property of anti-DNA Abs, which have a high number of positively charged amino acids, such as Arg and Lys, in the complementarity-determining regions (CDRs) of variable domains [7–10]. Thus, similar to CPPs, non-specific electrostatic interactions of anti-DNA Abs with negatively charged cell surface molecules, such as heparin sulfate proteoglycans, have been proposed to contribute to their cell-penetrating activity without cell-type specificity [2, 10, 11]. Despite numerous observations of the cell-penetrating activity of anti-DNA Abs, their specific endocytic pathways are poorly studied. It is likely that one of the endocytic pathways involved in the internalization of CPPs or other protein cargos, such as macropinocytosis, clathrin-mediated endocytosis, and caveolae/lipid-raft-mediated endocytosis [2, 12, 13], plays a role in the internalization of anti-DNA Abs [1, 14]. Notably, the cell-penetrating anti-DNA Abs reported so far eventually localized in the nucleus of cells, regardless of cells types and effects on a variety of cellular functions [14–16].

Despite the ability of anti-DNA Abs to penetrate into cells, detailed intracellular trafficking routes and cytotoxic mechanisms have not been well studied. Previously, we have reported an anti-DNA single chain variable fragment (scFv) Ab, 3D8 scFv, which binds and hydrolyzes DNA without significant sequence specificities [17]. In the present work, we investigated the endocytic pathway and intracellular trafficking of 3D8 scFv in HeLa cells, and underlying mechanism for cytotoxicity by 3D8 scFv. Our results demonstrated that 3D8 scFv internalizes by caveolae/lipid raft pathway-mediated endocytosis through initial interactions with heparin sulfate proteoglycans on cell surface and accumulates in the cytosol without translocation to nucleus, thereby inducing apoptotic cell death by its capability to degrade cellular RNAs. To our best knowledge, this is the first report on cell-penetrating anti-DNA Ab which accumulates in the cytosol without further trafficking into the nucleus.

Materials and methods

Cell culture. Adherent human cancer cell lines, HeLa, HCT116, and U87MG, were purchased from ATCC (Manassas, VA) and cultured in DMEM (Dulbecco's Modified Eagle Medium) supplemented with 10 % (v/v) fetal calf serum, 100 units/mL penicillin, and 100 μg/mL streptomycin (Invitrogen) in a humidified 5 % CO_2 / 95 % air atmosphere at 37 °C.

Antibodies and reagents. Heparin, chloropromazine, methyl-β-cyclodextrin (MβCD), cytochalasin D, and nocodazole (#M1404), TRITC-anti-rabbit IgG (#T6778) were purchased from Sigma (St Louis, MO). Alexa 488-transferrin (#T-13342**)**, Alexa 488-cholera toxin B (#C-22841), fluorescein isothiocyanate (FITC)-dextran (#D-1822), hoechst 33342 (#H1399), and lysotracker-red (#L7528) were obtained from Invitrogen. Anti-caveolin-1 (#610406) and FITC-anti-calnexin (#611862) Abs were from BD Biosciences. Anti-clathrin (#ab 14399), FITC-anti-mouse IgG (#ab 6785–1), and anti-58K Golgi protein (#ab 6284) Abs were obtained from Abcam. Anti-EEA1 (#sc-53939) and FITC-anti-rabbit IgG (#sc-2012) were purchased from Santa Cruz Biotechnology. Anti-dynamin (#VAM-SV041) was from Stressgen Biotechnologies. Anti-poly ADP-ribose polymerase (PARP) (#9542) and anti-β-actin (#4967) was from Cell signaling Tech. HRP-anti-rabbit IgG (#81–6120) was from Zymed laboratories. Cy3-conjugated anti-mouse IgG (#715-165-150) was from Jackson Laboratory. Polyclonal rabbit anti-3D8 scFv was produced by immunization in our laboratory.

3D8 scFv preparation. Mouse-originated 3D8 scFv protein was bacterially expressed and purified by IgG-sepharose affinity chromatography, according to the previously described procedures [17]. The protein concentrations were determined using extinction coefficients of 1.995 for scFv in units of mg $ml^{-1} \cdot cm^{-1}$ at 280 nm, which were calculated from the amino acid sequence.

Confocal microscopy. Cells were seeded at a density of 5×10^4 cells/well in 24-well plate over glass coverslips the day before use, and pre-incubated in serum-free DMEM for 30 min at 37 °C prior to treatment by proteins and/or reagents. Cells were incubated with 3D8 scFv for the indicated times in the presence of absence of pre-treatment with reagents at 37 °C. After stopping cellular uptake by adding three volumes of ice-cold PBS, cells were washed twice with cold PBS, fixed with 2 % paraformaldehyde (PFA) in PBS for 10 min at room temperature (RT), and then permeabilized with Perm-buffer (1 % BSA, 0.1 % saponine, 0.1 % sodium azide in PBS) for 10 min at room temperature (RT). After blocking with 2 % BSA in PBS for 1 h, 3D8 scFv-treated cells were incubated with rabbit anti-3D8 scFv Ab, followed by TRITC (or FITC)-anti-rabbit Ig. Nuclei were stained with Hoechst 33342 during the last 10 min of incubation at RT. Cells on coverslip were mounted in Vectashield anti-fade mounting medium (Vector Labs), and observed with Zeiss LSM 510 laser confocal microscope and analyzed with Carl Zeiss LSM Immage software.

In experimentation with soluble heparin, HeLa cells were pre-treated with 100 IU/ml heparin for 30 min at 37 °C and then incubated with 3D8 scFv (10 μM) or Alexa 488-transferrin (10 μg/ml) for 2 h at 37 °C, prior to cell fixation and permeabilization. In experimentation with endocytosis markers, HeLa cells were co-treated with 3D8 scFv (10 μM) and either Alexa 488-transferrin (10 μg/ml), Alexa 488-Ctx-B (10 μg/ml), or FITC-dextran (10 μg/ml) for 2 h at 37 °C, prior to cell fixation and permeabilization. In experimentation with inhibitors for endocytic pathways, HeLa cells were incubated with 3D8 scFv (10 μM) for 2 h at 37 °C with or without pre-treatment of chloropromazine (10 μg/ml), MβCD (5 mM), or cytochalasin D (1 μg/ml) for 30 min at 37 °C, followed by cell fixation and permeabilization. In pulse-chase experiments, HeLa cells were incubated with 3D8 scFv (10 μM) for 2 h or Alexa 488-labeled transferrin (10 μg/ml) for 30 min at 37 °C, quickly washed twice with PBS, and then incubated further at 37 °C for the specified time in the Result section. After washing, fixation, and permeabilization of cells, images were detected by incubation with FITC-anti-calnexin, anti-3D8 scFv, anti-caveloin, anti-EEA1, or anti-58k Golgi protein followed by the appropriate secondary Abs conjugated to TRITC, Cy3, or FITC. In case of nocodazole treatment, HeLa cells were incubated with 3D8 scFv (10 μM) for 2 h, prior to incubation with 20 μM nocodazol for 30 min at 37 °C and then cultured for 3.5 h at 37 °C.

Flow cytometry. HeLa cells grown in six-well plates ($1x10^5$ cells/well) were pre-incubated in serum-free DMEM for 30 min at 37 °C and were left untreated or treated with each inhibitor for 30 min at 37 °C before 3D8 scFv (10 μM) treatment. Suspended cells with trypsin were treated once more with 0.1 % trypsin for 3 min at 37 °C to wash off the surface-bound protein. After washings with ice-cold PBS once, cells were fixed and permeabilized as per the procedures described above, "confocal microscopy". Cells were washed with ice-cold PBS twice, labeled with anti-rabbit 3D8 scFv Ab followed by TRITC-anti-rabbit, and then analyzed using a Becton Dickinson FACSCalibur™ (BD Biosciences). For each test, $1x10^4$ cells were analyzed.

RNA interference. Small interfering RNA (siRNA) oligonucleotides were synthesized at Bioneer Co. (Daejeon, Korea). The mRNA sequences targeted by caveolin-1, clathrin, and dynamin-2 siRNA were 5'-AGA CGA GCU GAG CGA GAA GCA -3' [18, 19], 5'- AAC CUG CGG UCU GGA GUC AAC -3' [20], and 5'- GUG GAC CUG GUU AUC CAG GAG CUA A -3' [21] respectively. An unrelated (scramble) siRNA with sequence of 5'- CCU ACG CCA CCA AUU UCG U -3' was employed as a control. HeLa cells grown to 50 % confluency on a six-well or 24-well plate were transfected with siRNA using Lipofectamine 2000 (Invitrogen), according to the manufacturer's instruction. After 48 h, cells on six-well plate were used for immunobottings using anti-caveolin, anti-clathrin, or anti-dynamin Ab and fluorescent images in the cells on the 24-well plate were analyzed with confocal microscopy as described above.

FRET-based RNA-cleavage assay. FRET (Fluorescence resonance energy transfer)-based nucleic acid-hydrolysis assay [22] was carried out to detect RNA-hydrolyzing activity in live cells. HeLa cells were incubated with 3D8 scFv (10 μM) for 2 or 24 h. After washing, cells were transfected with 21-base length of RNA substrate labeled with 6-carboxyfluorescein (FAM) at the 5'-terminus and a black hole quencher (BHQ) at the 3'-terminus (that is 5' FAM -CGAT-GAGTGCCATGG ATATAC- BHQ 3') that was generated by M-biotech. The oligonucleotides (200 nM) were delivered by Lipofectamine 2000 transfection reagent into HeLa cells grown in a black 96-well plate. Immediately after transfection, the fluorescence intensity was read for 2 h in real-time by a fluorescence detector (Molecular Devices).

RNA integrity analysis. Total cellular RNA was extracted from cells, using the Trizol (Gibco Invitrogen), according to the manufacture's instruction. Aliquots (1–5 μg) of total RNA were either directly resolved on 1 % agarose gel or used for first strand cDNA synthesis using PreMix cDNA synthesis kit (Bioneer, Korea) and oligo dT primer. From cDNA template, transcripts specific for GAPDH and β-actin were amplified by RT-PCR. The PCR products were then applied to agarose gel electrophoresis followed by ethidium bromide staining.

RNA cleavage assays with purified 3D8 scFv. 3D8 scFv (0.1 μM) or HW1 scFv (0.1 μM) purified from bacterial expression [17, 23] was incubated with total cellular RNA (1 μg) extracted from HeLa cells, in TBS buffer (50 mM Tris-Cl, pH 7.5, 50 mM NaCl, pH 7.5) at 37 °C for 2 h prior to detection of hydrolysis. RNase A (1 U) was used as a positive control in the buffers provided by the manufacturer (New England Biolabs). RNase-free reagents were used in all procedures.

Cell viability assays. Cells seeded at density of 5×10^3 cells/well in 96-well plates were cultured overnight and then treated with 0–40 μM of 3D8 scFv for 48 h. Cell viability was determined using a colorimetric MTT [3-(4,5-dimethylthiazol-2-yl)-2,5-diphenyltetra-

zolium bromide]-based Cell Growth Determination kit (Sigma) [23].

DNA fragmentation analysis. DNA fragmentation was analyzed as previously described [24] with slight modifications. HeLa cells were incubated with 3D8 scFv (10 μM) for 48 h at 37 °C (5×10^5 cells/lane), and soluble DNA was then extracted from the cells using genomic DNA purification kit according to the manufacturer's guide (Qiagen). Extracted DNA was resolved on 2% agarose gel and visualized by ethidium bromide staining.

Western blotting. Cells (3×10^5 cells/well) were seeded in six-well plates, grown overnight, and then treated with 3D8 scFv under conditions as indicated in the figure legends. The Western blotting was then performed as described previously [23]. The appropriate secondary antibodies conjugated to horse radish peroxidase were used for developing chemiluminescence (Amersham Pharmacia Biotech).

Results

3D8 scFv translocates across the plasma membrane and accumulates in the cytosol of cells. We investigated the ability of 3D8 scFv to penetrate into cells in human cervical cancer HeLa cells, which have been extensively used as a model cell line for CPPs and anti-DNA Abs [1, 25]. The cells were incubated with 3D8 scFv protein (1, 5, 10, and 20 μM) for various periods of time (0.5–12 h) at 37 °C, and then treated with trypsin to remove surface bound proteins before fixing and staining cells. After immunofluorescent labeling of 3D8 scFv, the level of 3D8 scFv taken up by the cells was quantified by flow cytometry (Fig. 1). The internalization of 3D8 scFv increased in a concentration-dependent manner, reaching a plateau after ~2 h for the concentrations tested (Fig. 1A, B). The time-course analysis of subcellular localization of 3D8 scFv by confocal fluorescence microscopy revealed that it was retained in punctate, endosome-like vesicles in the cytosol between 0.–2 h and then diffused throughout the cytosol up to 48 h with little accumulation in the nucleus (Fig. 1C). This is quite a surprising observation because cell-penetrating anti-DNA Abs reported so far eventually accumulated in the nucleus, usually within a few hours of internalization [3, 10, 11, 14, 26]. The majority of CPPs, such as Tat and arginine-rich peptides, also preferentially localize in the nucleus [2]. Efficient intracellular entry and cytosolic accumulation of 3D8 scFv were also observed in other human cancer cells, such as of HCT116 (colon carcinoma) and U87MG (glioma) (Fig. Supp. 1), suggesting that the cell-penetrating ability of 3D8 scFv is not cell-type specific, as some anti-DNA Abs and CPPs are [2]. Cellular entry of 3D8 scFv was not observed at all when it was incubated with cells up to 2 h at 4 °C (data not shown), suggesting that 3D8 scFv internalization is an energy-dependent process [2, 25].

The next question was: What are the cell surface receptors for the initiation of internalization of 3D8 scFv? Previous reports have shown that, prior to internalization, positively charged anti-DNA Abs and CPPs have been shown to interact electrostatically with the extracellular matrix on the cell surface through binding mainly to the negatively-charged proteoglycans, such as heparan sulfate [2, 25]. Therefore, to explore whether internalization of the basic 3D8 scFv (pI = 9.15) is also initiated by electrostatic binding to ubiquitous proteoglycans, HeLa cells were pre-incubated for 30 min with heparin (100 IU/ml), as a soluble competitor, prior to incubation with 3D8 scFv (10 μM) for another 2 h. Confocal microscopy revealed that heparin completely blocked the internalization of 3D8 scFv as well as cell surface binding (Fig. 1D). Complete blocking of 3D8 scFv internalization by heparin was also observed in human cancer cells of HCT116 and U87MG (Fig. Supp. 1). On the other hand, heparin did not affect the translocation of Alexa 488-transferrin (Fig. 1D), which is internalized by initial interaction with its specific transferrin receptor on the cell surface [2]. Thus, it is very likely that 3D8 scFv interacts with negatively charged proteoglycans prior to internalization, similar to anti-DNA Ab, F4.1 [11].

3D8 scFv internalization is mediated by caveolae/lipid raft endocytosis. For the initial periods of internalization, 3D8 scFv were retained in the punctate, endosome-like compartments (Fig. 1B, C). To elucidate the specific internalization mechanism of 3D8 scFv, 3D8 scFv were stained with FITC-labeled intracellular trafficking tracers for the three major endocytic pathways, such as transferrin (TF) for clathrin-mediated endocytosis, cholera toxin-B (Ctx-B) for caveolae/lipid raft-mediated endocytosis, and dextran for macropinocytosis [2, 25]. Results showed that the 3D8 scFv-containing compartments were colocalized with Ctx-B, but neither with transferrin nor dextran, as visualized after co-treatment of HeLa cells with 3D8 scFv and trafficking makers for 2 h at 37 °C (Fig. 2A). The internalization mechanism of 3D8 scFv was further investigated using pharmacological inhibitors to interfere with the above mentioned three individual endocytic pathways. The inhibitors were chlorpromazine to inhibit clathrin-dependent endocytosis by preventing the recycling of clathrin, methyl-β-cyclo-

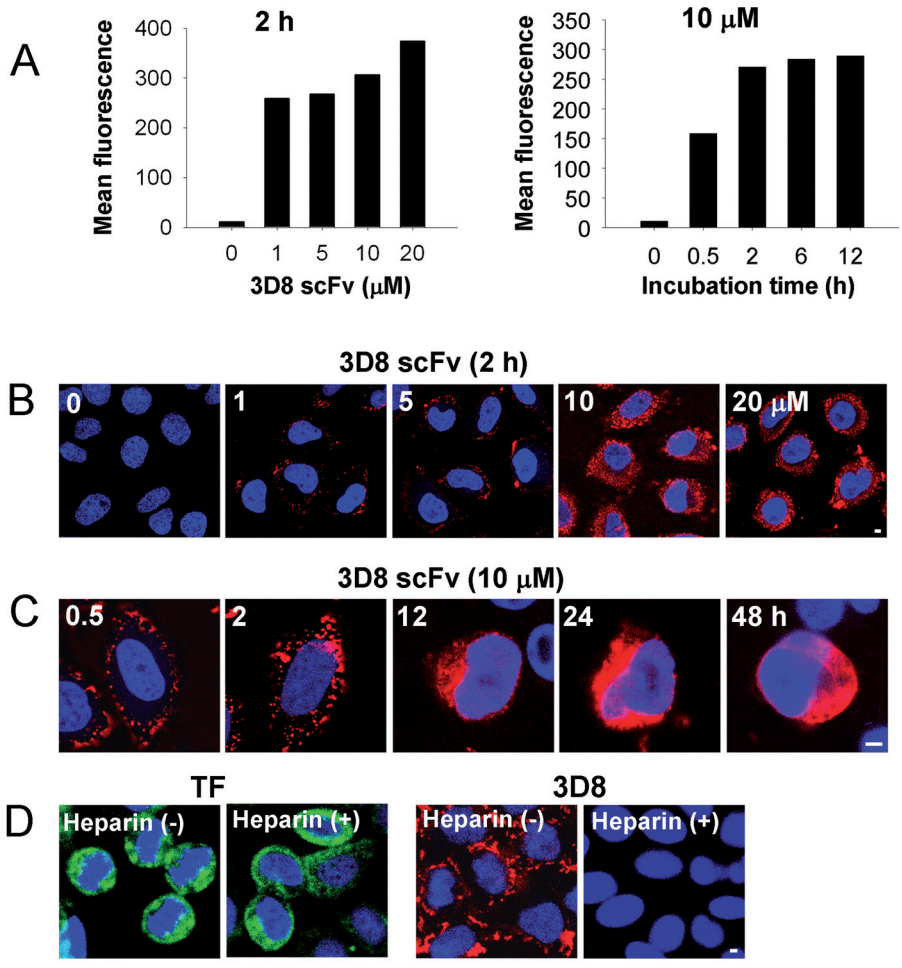

Figure 1. 3D8 scFv penetrates into cells by its interaction with heparin sulfate proteoglycans on the cell surface and localizes in the cytosol. (*A*) Quantification of 3D8 scFv uptake as a function of its concentrations (0–20 μM) for 2 h (*left panel*) or at 10 μM for the various periods (*right panel*), which was analyzed by flow cytometry and expressed by mean fluorescence intensity. (*B, C*) Fluorescent images of internalized 3D8 scFv at various concentrations (0–20 μM) for 2 h (*B*), or at 10 μM for the various periods (*C*), which was analyzed by confocal fluorescence microscopy. In (*A-C*), HeLa cells incubated at 37 °C with 3D8 scFv for the indicated concentrations and periods were fixed, permeabilized, and then stained with rabbit anti-3D8 scFv Ab followed by secondary TRITC-anti-rabbit IgG (red) before flow cytometric or confocal microscopic analyses, as described in detail in the methods. (*D*) Inhibition of 3D8 scFv internalization by soluble heparin treatment. HeLa cells were incubated with 3D8 scFv (10 μM) or Alexa 488-labeled transferrin (TF) (10 μg/ml) for 2 h with or without pre-treatment of soluble heparin (100 IU/ml) for 30 min. In (B-D), Blue color depicts Hoechst 33342-stained nuclei. Scale bar, 5 μm.

dextrin (MβCD) to inhibit caveolae/lipid raft endocytosis by depleting cholesterol in cell membranes, thus preventing the formation of caveolae, and cytochalasin D to inhibit macropinocycosis by disrupting actin microfilaments [25]. HeLa cells were pre-treated with these specific inhibitors for 30 min at 37 °C, prior to the addition of 3D8 scFv (10 μM). As shown in Figure 2B and C, confocal microscopic and flow cytometric analyses revealed that pre-incubation of cells with MβCD (5 mM), but neither with chlorpromazine (10 μg/ml) nor cytochalasin D (1 μg/ml), led to a significant reduction in the amount of 3D8 scFv internalized. These results strongly indicated that 3D8 scFv is internalized via caveolae/lipid raft-mediated endocytosis, in a way similar to that of anti-DNA mAb H7 [14].

Next, we carried out knock-down experiments of genes involved in the caveolae/lipid raft-mediated endocytosis using siRNA techniques. Caveolin-1 (cav-1) is an essential component for both the structure and function of caveolae, called a specialized lipid rafts containing caveolin [13]. To verify caveolin-dependency of 3D8 scFv endocytosis, HeLa cells were transfected with cav-1 siRNA or control siRNAs (clathrin- or scramble siRNA), and incubated with 3D8 scFv for 2 h after 48 h of transfection. Western blotting analysis revealed that cav-1 and clathrin expression levels were reduced by 50% and 70%, respectively (Fig. 3A). Cav-1 depletion significantly inhibited the endocytosis of 3D8 scFv, compared to that of the control cells treated with scramble siRNA, indicative of the essential role of cav-1 played in 3D8 scFv endocytosis (Fig. 3B). However, there was no significant effect of reduced expression of clathrin on the 3D8 scFv endocytosis, excluding the involvement of clathrin-mediated endocytosis for 3D8 scFv. Since endocytosis via caveolae is a GTPase dynamin-dependent process [27] and a dynamin is essential for helping pinch the endocytic vesicle off from the plasma membrane [27], we also examined involvement of dynamin in 3D8 scFv endocytosis. Figure 3C shows that colocalization of 3D8 scFv with dynamin was mostly seen at the plasma membrane during short time (30 min) incubation, as expected. Dynamin depletion by siRNA transfection completely inhibited intracellular uptake of 3D8 scFv (Fig. 3D, E). Taken

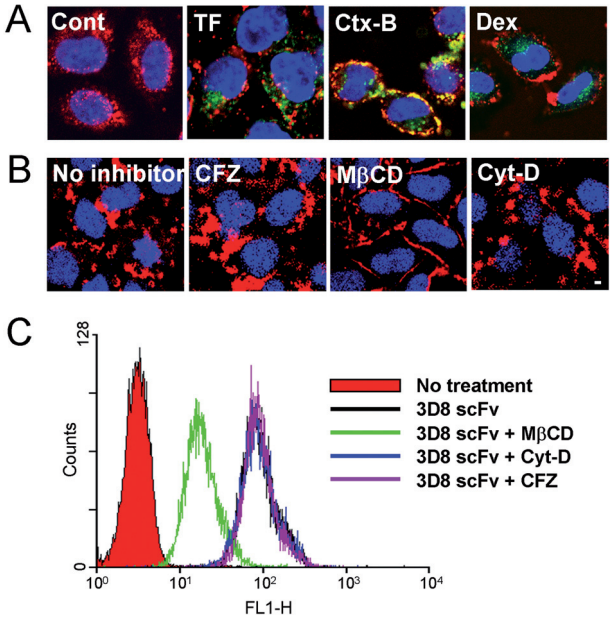

Figure 2. 3D8 scFv enters the cells via caveolae/lipid raft-mediated pathway. (*A*) Co-localization of 3D8 scFv with intracellular endocytic markers. HeLa cells were co-treated with 3D8 scFv (10 μM) (red) and Alexa 488-transferrin (TF, green), Alexa 488-choleratoxin-B (Ctx-B, green), or FITC-dextran (Dex, green) for 2 h and then analyzed by confocal microscopy as described in detail in the methods. Cells treated only with 3D8 scFv were also shown as a control (Cont). In (*A, B*), nuclei were costained with Hoechst 33342 (blue). (*B, C*) Effects of pre-treatment of specific endocytosis inhibitors on the 3D8 scFv cellular uptake, which were analyzed by confocal microscopy (*B*) or flow cytometry (*C*). HeLa cells were incubated with 3D8 scFv (10 μM) for 2 h with or without pre-treatment of chloropromazine (CFZ, 10 μg/ml), MβCD (5 mM), and cytochalasin D (Cyt-D, 1 μg/ml) for 30 min. Then, the subcellular localization (*B*) and cellular internalized level (*C*) of 3D8 scFv were analyzed by immunofluorescent staining with anti-3D8 scFv and TRITC-labeled anti-rabbit IgG. Scale bar, 5 μm.

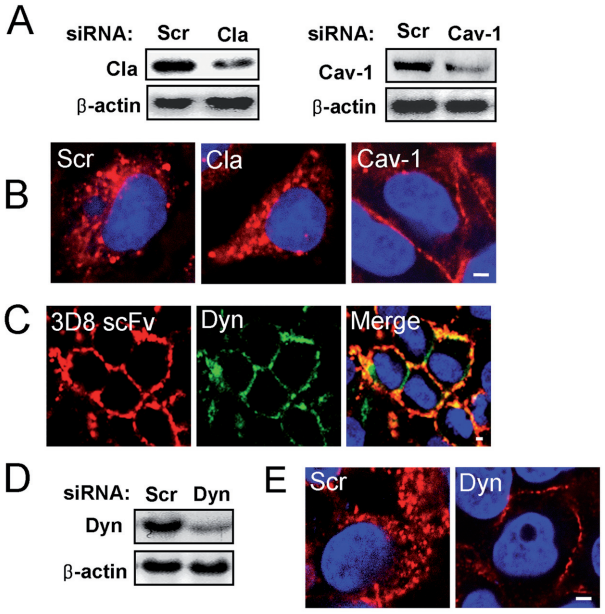

Figure 3. 3D8 scFv endocytosis is dependent on caveolin-1 and dynamin. (*A, D*) Western blots to monitor the expression levels of clathrin (Cla) (*A*), caveolin-1 (Cav-1) (A), or dynamin (Dyn) (*D*) in HeLa cells transiently transfected with the specific siRNA against each gene. (*B, E*) Effects of knocking-down clathrin (Cla) (*B*), caveolin-1 (Cav-1) (*B*), or dynamin (Dyn) (*E*) by the specific siRNA against each gene on the uptake of 3D8 scFv in HeLa cells. At 48 h after transfection with the specified siRNAs, HeLa cells were incubated with 3D8 scFv (10 μM) for 2 h and then visualized by confocal microscopy. In (*A, B, D, E*), controls cells treated with a scrambled siRNA (Scr) are also shown. (*C*) Co-localization of 3D8 scFv (red) with dynamin (Dyn, green) in HeLa cells treated with 3D8 scFv (10 μM) for 2 h was monitored by confocal microscopy. In (*B, C, E*), blue color depicts Hoechst 33342-stained nuclei. Scale bar, 5 μm.

altogether with the observations characterized by clathrin-independence, dynamin-dependence, and sensitivity to cav-1 knock-down and cholesterol depletion led us to conclude that the cellular internalization of 3D8 scFv is mediated by caveolae/lipid raft endocytosis [27, 28].

3D8 scFv is released into cytosol directly from caveolae/caveosomes. As shown in Figures 1–3, 3D8 scFv internalized via caveolae/lipid raft endocytosis were retained in punctate, endosome-like vesicles in the cytosol, between 0.5–2 h and then diffused throughout the cytosol with little accumulation in the nucleus. To follow up the intracellular trafficking routes of 3D8 scFv, we carried out pulse-chase experiments. HeLa cells were incubated with 3D8 scFv for 30 min, washed to remove extracellular bound 3D8 scFv, and then fluorescently costained with Abs against 3D8 scFv and cav-1 at 0, 2, 4, 6, and 12 h. Time-course trafficking of both 3D8 scFv and cav-1 revealed that 3D8 scFv were seen in punctate compartments on the plasma membrane immediately after 3D8 scFv treatment (0 h), then traversed toward inside the cytosol up to 2 h together with cav-1, and then diffused throughout the cytosol after 4 h, simultaneously separating completely from cav-1 signal (Fig. 4). Thus, cav-1 showed the route similar to that of 3D8 scFv for the earlier period (0–4 h). However, after 4 h of 3D8 scFv internalization, cav-1 signal significantly disappeared, implying that caveosomes eventually take the degradative pathway of late endosomes and lysosomes. This observation is in good agreement with a previous report that caveosomes formed by internalization of albumin in human HepG2 cells were degraded after 3 h of internalization by fusion with lysosomes [29]. However, it should be noted that 3D8 scFv was not degraded at all even after caveosome degradation (Fig. 4), suggesting that 3D8 scFv escapes from caveolae/caveosome to translocate into the cytosol.

Next, we further examined whether the cytosolic release of 3D8 scFv from caveolae/caveosome re-

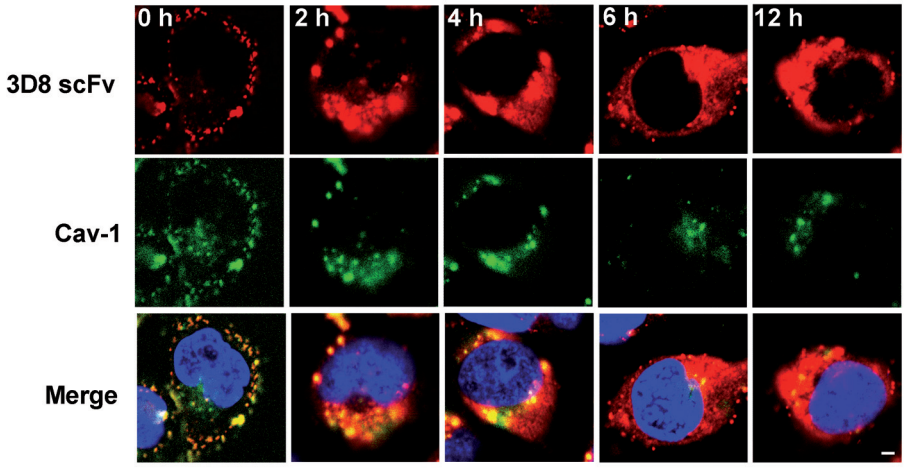

Figure 4. 3D8 scFv translocates from caveloae/caveosome to the cytosol. The time-course distributions of 3D8 scFv (upper panels, red), caveolin-1 (Cav-1) (middle panels, green), and their colocalization (lower panels) in HeLa cells were visualized with confocal microscopy. HeLa cells were incubated with 3D8 scFv (10 μM) for 30 min, washed and then incubated for the indicated times (0–12 h). Following fixation and permeabilization, cells were stained with primary Abs against 3D8 scFv and caveolin-1 (Cav-1), and then secondary Abs of TRITC-labeled anti-rabbit IgG for 3D8 scFv (red) and FITC-labeled anti-mouse IgG for Cav-1 (green) detections. Nuclei were costained with Hoechst 33342 (blue). Bar, 5 μm.

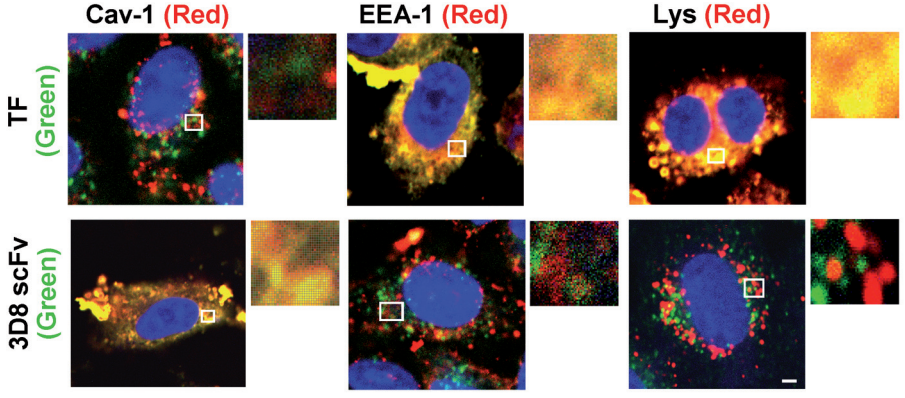

Figure 5. Internalized 3D8 scFv does not localize to the endosomal or lysosomal pathways. After incubated with either Alexa 488-labeled transferrin (TF, 10 μg/ml) for 30 min (*upper panels*) or 3D8 scFv (10 μM) for 2 h (*lower panels*), HeLa cells were washed immediately, fixed, and permeabilized. Then cells were stained with primary Abs against 3D8 scFv, caveolin-1 (Cav-1), or early endosomes (EEA-1) and then secondary Abs of FITC-labeled anti-rabbit IgG for 3D8 scFv (green), or Cy3-labeled anti-mouse IgG for Cav-1 and EEA-1 (red) detections. Late endosomes/lysosomes were stained with lysotracker-red (red). Merged images obtained by confocal microscopy are shown. Side frames show the selected areas of the images enlarged. Nuclei were costained with Hoechst 33342 (blue). Bar, 5 μm.

quires the fusion with early endosomes and late endosomes, or lysosomes. As uptake by caveosomes is a slower process than that by clathrin-coated pits [30], HeLa cells were incubated with 3D8 scFv for 2 h or transferrin for 30 min before being fixed and then fluorescently labeled with Abs against 3D8 scFv and EEA-1 (early endosomal antigen-1) or lysotracker-red, agent accumulated in late endosomes/lysosomes [31]. The resulting overlays revealed that the signal of 3D8 scFv merged with only that of cav-1, but not with EEA-1 and lysotracker-red, whereas transferrin that is delivered to early and/or late endosomes before being recycled to plasma membrane was colocalized with EEA-1 and lysotracker-red, but not with cav-1 (Fig. 5). These results indicated that 3D8 scFv escapes from caveosome into the cytosol, bypassing further endosome sortings and degradative lysosomal pathway. Up to 12 h-chase, colocalization of 3D8 scFv with markers for EEA-1 or lysotracker-red was not seen (data not shown).

Previous reports have shown that endosomal vesicles formed by internalization of some CPPs are transported into Golgi apparatus and ER within the cytosol before the release of CPPs from the vesicles into the cytosol [2]. To determine whether 3D8 scFv in caveolae/caveosomes is transported to endoplasmic reticulum (ER) and/or Golgi before its cytosolic accumulation, time-course chase of 3D8 scFv was

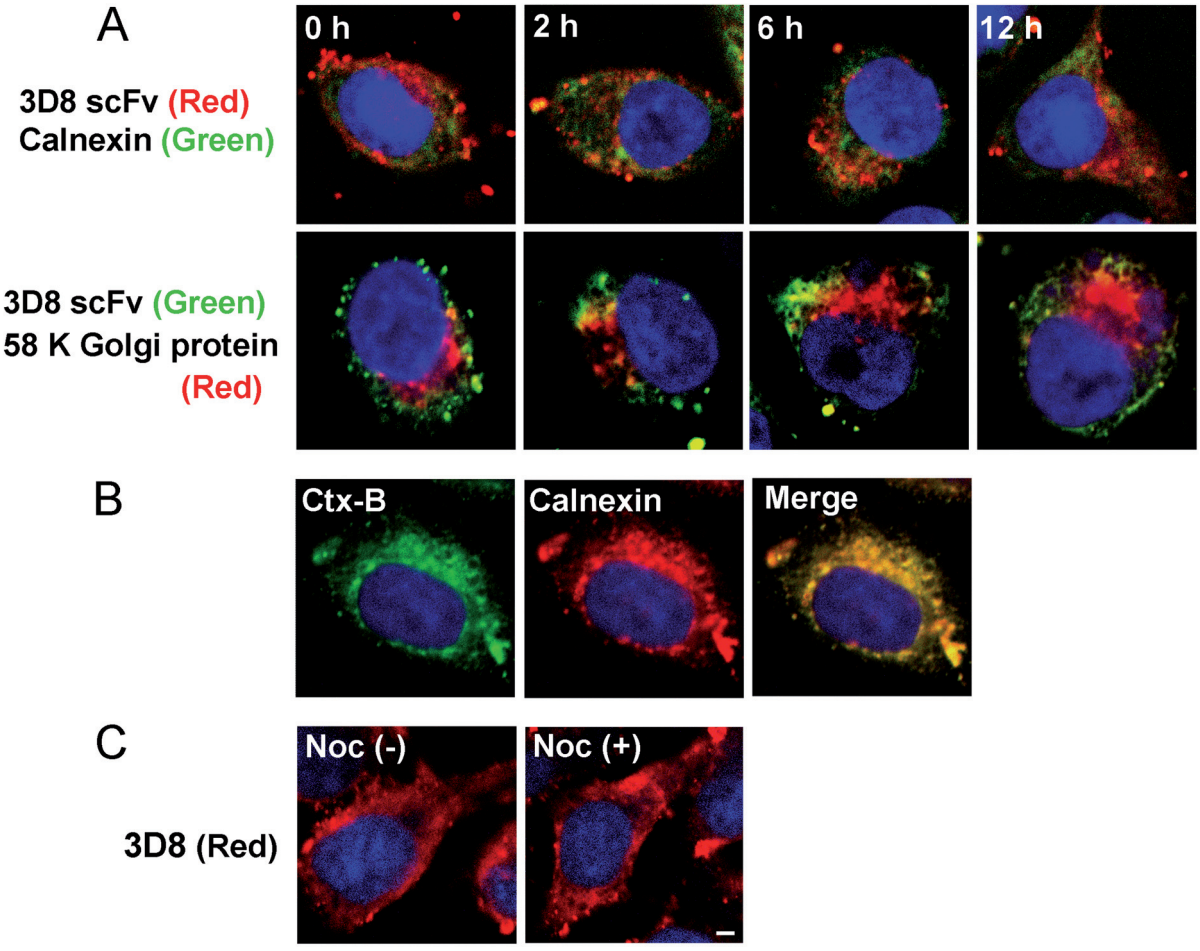

Figure 6. Endocytosed 3D8 scFv translocates directly into the cytosol, bypassing ER, Golgi, and other transporting vesicles. (*A*) Pulse-chasing experiments to monitor the co-localizations of 3D8 scFv with either the ER marker of calnexin, (*upper panels*) or the Golgi marker of 58K Golgi protein (*lower panels*). HeLa cells were incubated with 3D8 scFv (10 μM) for 30 min, quickly washed, and further incubated for the indicated periods. Following fixation and permeabilization, cells were stained with Abs against calnexin (green FITC signal), 58K Golgi protein (red Cy3 signal), or 3D8 scFv [red TRITC (*upper panels*) or green FITC (*lower panels*) signals], prior to confocal microscopic analyses. Overlayed confocal images are shown. (*B*) Colocalization of Ctx-B (green Alexa 488 signal) and calnexin (red Cy3 signal) for endocytosis period. HeLa cells were treated with Alexa 488-Ctx-B (10 μg/ml) for 2 h, stained with Ab against calnexin. (*C*) Effect of nocodazole (Noc) on translocation of 3D8 scFv into the cytosol. After incubation with 3D8 scFv (10 μM) for 2 h, cells remained untreated (*left panel*) or were treated with nocodazole (20 μM) for 30 min (*right panel*), followed by further incubation for 3.5 h. Nuclei were costained with Hoechst 33342 (blue). Scale bars correspond to 5 μm.

carried out with the subcellular organelle markers; calnexin for ER and 58K Golgi protein for Golgi. As shown in Figure 6A, 3D8 scFv was not colocalized with both ER and Golgi markers for up to 12 h of trafficking, whereas control Ctx-B, which is known to translocate to ER from caveosomes [13], overlapped with the ER marker within 2 h of trafficking (Fig. 6B). The effect of nocodazole on the cytosolic release of 3D8 scFv was further investigated. Nocodazole, a microtubule-depolymerzing agent, inhibits transport of caveolae/caveosomes into caveolin-free carrier vesicles which move rapidly along microtubules to eventually reach other subcellular vesicular organelles [32]. In the pulse-chase experiment, where cells were pulsed with 3D8 scFv (10 μM) for 2 h, treated with nocodazole (20 μM) for 30 min, and then incubated for another 4 h, nocodazole did not block the divergence of the internalized 3D8 scFv into the cytosol (Fig. 6C). These results indicate that internalized 3D8 scFv can be translocated directly into the cytosol from the caveosomes without traversing into cellular organelles and other intermediate vesicles.

Internalized 3D8 scFv triggers apoptotic cell death by hydrolyzing cellular RNAs. The prolonged incubation of cells after 3D8 scFv internalization exhibited cytotoxicity. Figure 7 shows the cytotoxicity of 3D8 scFv in human cancer cell lines of HeLa, HCT116, and U87MG when incubated with various concentrations of 3D8 scFv (5–40 μM) for 48 h. Cell viability was

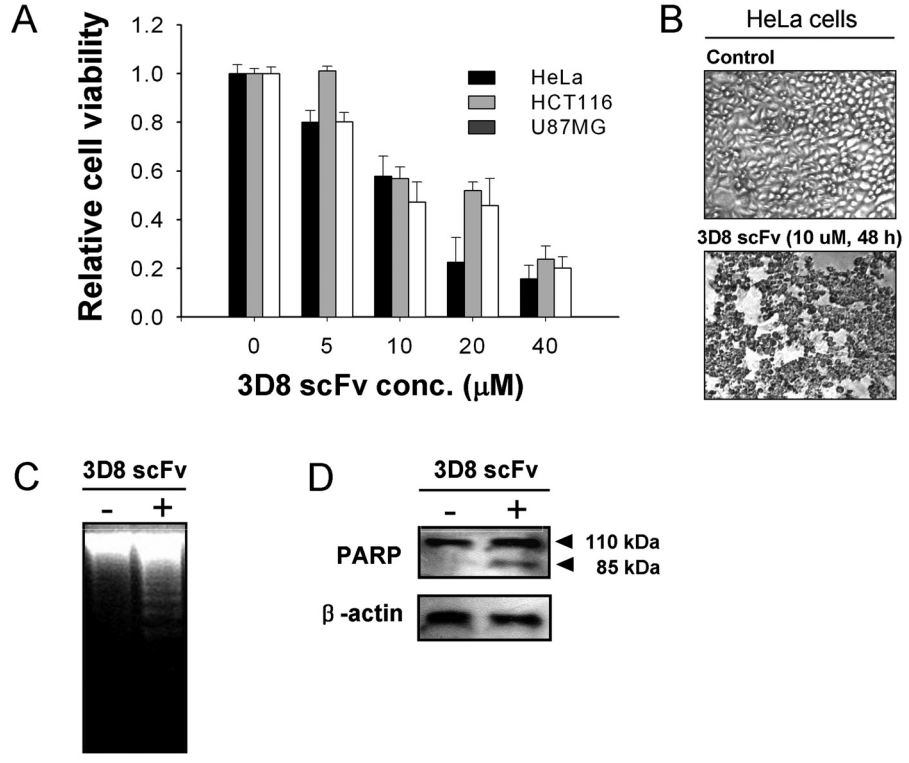

Figure 7. Endocytosed 3D8 scFv induces apoptotic cell death. (*A*) The viabilities of HeLa, HCT116, and U87MG cells treated with varying concentrations of 3D8 scFv for 48 h were determined by MTT assay and presented as the percentage of viable cells compared with the untreated control cells. Error bars indicate the standard deviations for at least triplicated experiments. (*B*) Phase-contrast microscopic images of HeLa cells untreated (*upper panel*) or treated with 3D8 scFv (10 μM) for 48 h (*lower panel*). (*C, D*) DNA fragmentation (*C*) and PARP activation (*D*) were detected by agarose gel electrophoresis and Western blotting, respectively, from the HeLa cells untreated or treated with 3D8 scFv (10 μM) for 48 h.

determined by MTT assay [23]. Compared to that of the untreated cells, the viability of three cell lines treated with 10 and 40 μM 3D8 scFv was decreased ~50–60 % and ~20 %, respectively (Fig. 7A). Dying cells became rounded and were detached from the bottom of culture plates (Fig. 7B). However, treatment of the cells with 1 μM 3D8 scFv exhibited no significant cytotoxicity up to 48 h of incubation (data not shown). Genomic DNA fragmentation with laddering pattern (Fig. 7C) and cleavage of poly (ADP-ribose) polymerase-1 (PARP-1) (Fig. 7D) demonstrated that 3D8 scFv induced apoptotic cell death.

Previous reports have shown that cell-penetrating anti-DNA Abs with DNA-hydrolyzing activity also showed cytotoxicity, triggering apoptosis in various cancer cells [3, 6]: anti-DNA Abs were internalized and accumulated in the nucleus, leading the authors to postulate that apoptotic cell death was triggered by damage to nuclear DNA [3, 6]. Unlike the above cell-penetrating anti-DNA Abs, however, the final destination of 3D8 scFv up to 48 h was the cytosol without accumulation in the nucleus (Fig. 1C). Thus, we hypothesized that cytotoxicity exerted by cytosolic 3D8 scFv was due to its ability to hydrolyze cytosolic RNAs, since many DNA-hydrolyzing Abs can also hydrolyze RNA [33] and some ribonucleases (RNases) give rise to cell toxicity when they are internalized into the cytosol [19, 34].

RNA-hydrolyzing activity of 3D8 scFv endocytosed in live cells was analyzed by FRET-based cleavage assay [22], in which the hydrolysis of the transfected ribonucleotides, that are double-labeled with a fluorophore at 5'-terminus and its quencher at 3'-terminus, can be read out with the increase in fluorescence intensity of the cells. HeLa cells were incubated with 3D8 scFv (10 μM) for 2 or 24 h, prior to transfection with double-labeled RNA substrate, and the intensity of fluorescence in the cells was measured in real-time for 2 h with 5-minute intervals by a fluorescence analyzer (Fig. 8A). Compared with untreated cells, cells treated with 3D8 scFv for 24 h, but not for 2 h, exhibited RNA-hydrolyzing activity. These results suggest that internalized 3D8 scFv does not exert RNA degradation until its release from its carrier caveolae/caveosomes into the cytosol (> 2 h, Fig. 1) and maintains its nuclease ability even in the reducing environment of the cytosol.

The ability of cytosolic 3D8 scFv to hydrolyze exogenous RNA substrate prompted us to investigate its hydrolyzing activity of cellular RNAs. After HeLa cells were incubated with 3D8 scFv (10 μM) for 24 h, the total cellular RNA was isolated and electrophoretically resolved on 1 % denaturing agarose gels. Integrity of 28S or 18S ribosomal RNA (rRNA) appeared to be intact, evidenced by ethidium bromide staining of the gel (Fig. 8B), indicating that rRNAs were not degraded by 3D8 scFv. To assess the damage

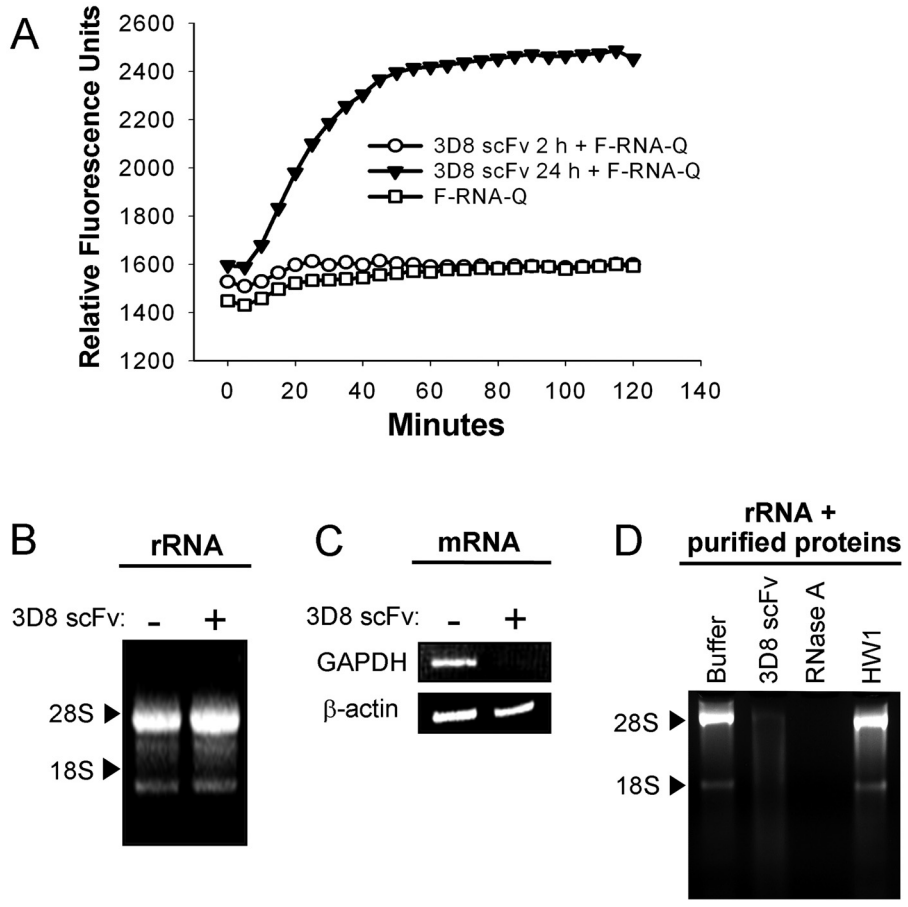

Figure 8. Cytosolically localized 3D8 scFv maintains its RNA-hydrolyzing activity and degrades cytosolic mRNA. (A) RNA-hydrolyzing activity of 3D8 scFv endocytosed into HeLa cells was monitored by FRET-based cleavage assay using the exogenous RNA substrate. Cells untreated or treated with 3D8 scFv (10 μM) for 2 or 24 h were transfected with 21-bp single stranded RNA substrate (F-RNA-Q, 200 nM), followed by recording of the fluorescence intensity in real-time for 2 h, as described in detail in Method. (*B, C*) Influence of endocytosed 3D8 scFv on cellular rRNA (*B*) and mRNA (*C*) integrity. After HeLa cells were incubated with or without 3D8 scFv (10 μM) for 24 h, their total cellular RNA was extracted and used for either agarose gel elecrophoresis (*B*) or for cDNA synthesis, followed by PCR analysis using specific primers to GAPDH and β-actin genes (*C*). (*D*) RNA-hydrolysis activity of the purified 3D8 scFv from *E.coli.* The purified 3D8 scFv (0.1 μM) and HW1 scFv protein (0.1 μM) from *E.coli* supernatant and RNase A (1 U) were incubated with total cellular RNA (1 μg) extracted from HeLa cells at 37 °C for 2 h prior to electophoresis on an agarose gel.

to mRNA by 3D8 scFv, the abundance of mRNAs of two house-keeping genes, GAPDH and β-actin, was analyzed by RT-PCR using gene-specific primers after cDNA synthesis from the same total cellular RNA isolates. The losses of GAPDH and β-actin mRNAs were clearly detected, since the relative abundance of GAPDH and β-actin mRNAs was decreased completely to 0 % and partially to 60 % of the control cells, respectively (Fig. 8C). These results indicate that cellular mRNAs were sensitive to endocytosed 3D8 scFv *in vivo*, compared to rRNAs. Intense degradation of rRNA (28S and 18S) was observed when rRNA purified from cells was incubated with 3D8 scFv (0.1 μM) in a test tube, but not when incubated with HW1 scFv, which is an irrelevant scFv purified from bacterial cells [23] using exactly the same procedures (Fig. 8D), confirming that 3D8 scFv possessed the RNase activity. Taken altogether, it is most likely that cytosolic 3D8 scFv that has escaped from its carrier caveolae/caveosomes hydrolyzes cellular RNAs, mainly mRNAs, leading to apoptotic cell death in various cancer cells.

Discussion

Many anti-DNA Abs have been shown to have cell-penetrating activity; however, their specific endocytic pathways have not been studied in detail, except anti-DNA mAb H7, which was internalized by caveolar endocytosis [14], as was 3D8 scFv. Caveolae, which are ubiquitously present in many vertebrate cell types, are generated by caveolin oligomerization and association of caveolin with cholesterol-rich lipid-raft do-

mains [13]. Caveolar vesicles budded from the plasma membrane can recycle back to the plasma membrane or fuse with caveosomes and/or early endosomes for delivery to various subcellular organelles (e.g., late endosomes, ER, and/or Golgi) [12, 13]. Caveosomes are non-degradative endosomal compartments with neutral pH and contain a caveolae marker (cav-1), lacking classic endosomal markers [13, 28]. SV40 virus and Ctx-B are well-known for their caveolar endocytosis and then merging with caveosome before further sorting to ER and/or Golgi [13, 28, 32]. 3D8 scFv internalized by caveolar endocytosis was colocalized with Ctx-B (Fig. 2A), indicating that a 3D8 scFv-containing caveolae vesicle fuses with caveosome. However, unlike Ctx-B (Fig. 6B) and SV40 [32], 3D8 scFv-containing caveolae/caveosomes did not translocate to early endosomes, late endosome/lysosomes (Fig. 5), ER or Golgi (Fig. 6A). Instead, 3D8 scFv appeared to escape directly into the cytosol from the caveolae/caveosome compartments before their degradation (Fig. 4). Notably, to the best of our knowledge, the cargos that directly translocate to the cytosol from caveolae/caveosome have not yet been reported. For anti-DNA mAb H7, its direct release from caveosomes to the cytosol before entering into the nucleus was proposed, but detailed trafficking studies were not performed [14]. Ctx-B and albumin are known as representative proteins internalized via caveolae, upon binding to a lipid-based receptor sphingolipid GM1 and albumin-binding adaptor protein (gp60) at plasma membrane, respectively. However, their post-caveosomal trafficking has not been well described, except for several studies showing that Ctx-B is transported to the Golgi complex (Fig. 6B), possibly through early endosomes [12, 27, 30]. Another interesting observation in the present study is microtubule-independency for the translocation of 3D8 scFv from the caveolae/caveosome into the cytosol (Fig. 6C). Previously nocodazole, a microtubule depolymerizing agent, was found to confine SV40 in caveolae/caveosome compartments, inhibiting its further trafficking into ER [32].

Escape of some CPPs or viruses from early/late endosomes into the cytosol before its merging with lysosomes depends on acidification of endosomes. The acidic pH in the endosome alters the conformation of the CPPs or the N-terminal region of influenza virus hemagglutinin-2 (HA2) to induce destabilization of lipid membranes, facilitating the escape from the endosomes into the cytosol [35]. At this point, the exact mechanism of how 3D8 scFv escapes from caveolae/caveosome compartments into the cytosol, while maintaining its biochemical activity, is not clear. However, at least the feature of neutral pH in the lumen of caveolae/caveosome compartments, distinguished from early/late endosomes, could exclude the possibility that 3D8 scFv escapes from caveolae/caveosomes into the cytosol by virtue of its conformational alteration in a low pH environment. There are, however, two possibilities: one is 3D8 scFv-containing caveolae/caveosomes recruit some proteins, which eventually destabilize to lyse the vesicles before its further trafficking into lysosomes, Golgi and/or ER. Recruiting some enzymes into caveosomes has been reported for glypican-1-containing caveosomes, such as heparanase, although how this is achieved is not well understood [36]. The other possibility is direct lysis of caveolae/caveosomes by 3D8 scFv. As described earlier, caveolae/caveosomes are mainly composed of caveolin and cholesterol-rich lipid-raft domains, where caveolin interactions with cholesterol through the conserved cationic and hydrophobic residues in the N-terminus of caveolin is important for the vesicle stability [13, 28]. Therefore, we can assume that 3D8 scFv with multiple basic residues is likely to interfere with the interactions between cholesterol and caveolin, thereby inducing disassembly of the vesicles. However, the detailed molecular basis of 3D8 scFv escape from the caveolae/caveosomes remains to be determined.

All of the cell-penetrating anti-DNA Abs reported so far are preferentially localized in the nucleus, similar to CPPs or CPP-conjugated proteins [2]. Common features of anti-DNA Abs that have a large number of positively-charged residues within CDRs of VH and/or VL domains due to their antigen binding properties, which resemble nuclear localization signal (NLS), have been attributed to their final accumulation within the nucleus of cells, like the CPPs [2, 7]. Peptides derived from CDRs of human or mouse anti-DNA Abs have been employed as a cell-penetrating carrier for nuclear delivery of plasmids or proteins [37–39]. However, 3D8 scFv was not translocated from the cytosol to the nucleus, remaining in the cytosol even up to 48 h after internalization. 3D8 scFv also has a large number of cationic amino acids in the VH- and VL-CDRs (total 4 Arg and 4 Lys residues) [17]. Three-dimensional structural analysis of the surface which is exposed to CDRs of 3D8 scFv reveals two patches clustered with basic amino acids; one is on VH-CDR3 (Arg94, Lys98, and Arg99 in Kabat numbering) and the other is on VL-CDR1 (Arg27 f, Arg28, and Lys29) [17]. Therefore, it is not clear why 3D8 scFv remained in the cytosol, although it shares common features of continuous or conformational clustering of basic amino acids with other cell-penetrating anti-DNA Abs or CPPs. 3D8 scFv binds to and hydrolyzes DNA and RNA without sequence specificity, but not proteins [17]. Accordingly, it is quite possible that 3D8 scFv binds to cytosolic RNAs

without sequence specificity, which may block further trafficking of 3D8 scFv into the nucleus. No exact recognition motifs for nuclear transportation were found in 3D8 scFv when its amino acid sequence was analyzed by sequence alignments with those of well-known NLSs existing on many nuclear-transporting proteins. Thus, another possibility could be attributed to the absence of primary and three-dimensional structural recognition motif for nuclear transportation in 3D8 scFv.

Nuclear localization of anti-DNA Abs with a DNA-hydrolyzing property has been shown to induce apoptotic cell death in a variety of cells, and the underlying mechanism has been suggested to be damage to nuclear DNA [3–6]. In the present study, however, cell-penetrating 3D8 scFv also induced apoptotic cell death by degrading cellular RNAs, mainly mRNA, but not nuclear DNA, due to their accumulation in the cytosol (Figs. 7, 8). It should be noted that some RNAses with cell-penetrating activity, such as Onconase and bovine seminal RNase, also induced apoptotic cell death by damaging cytosolic RNAs [34, 40].

The present work shows that 3D8 scFv translocates across the plasma membrane by caveolae/lipid-raft-mediated endocytosis upon interacting with anionic proteoglycans on the cell surface, accumulates in the cytosol, and then induces apoptotic cell death by hydrolyzing cellular RNAs. This is the first report of an anti-DNA Ab that localizes to the cytosol without reaching the nucleus and then induces apoptosis by its RNA-hydrolyzing activity. Besides, unlike previously reported anti-DNA Abs in intact IgG form, 3D8 traverses the plasma membrane in scFv format, lacking the constant regions of IgG, suggesting that the cell penetrating ability of anti-DNA Abs resides in VH and/or VL domain (s). Even though the exact molecular mechanism as to how 3D8 scFv escapes from the caveolae/caveosome into the cytosol is not clear yet, our results suggest that internalization mediated by caveolae may be a favorable pathway for cytotoxic drug delivery because it can avoid lysosomal degradation [13].

Electronic supplementary material. Supplementary material is available in the online version of this article at springerlink.com (DOI 10.1007/s00018-009-9179-2) and is accessible for authorized users.

Acknowledgements. This work was supported by grants from the Basic Research Program of the Korea Science & Engineering Foundation (R01-2006-000-10743-0), the Korean Health R&D project of the Ministry of Health and Welfare (01-PJ10-PG6–01 GN14–0007), and the BioGreen 21 Program (20070401034007) of the Rural Development Administration, Republic of Korea.

1 Ruiz-Arguelles, A., Rivadeneyra-Espinoza, L. and Alarcon-Segovia, D. (2003). Antibody penetration into living cells: pathogenic, preventive and immuno-therapeutic implications. Curr. Pharm. Des. 9, 1881–1887
2 Foged, C. and Nielsen, H. M. (2008). Cell-penetrating peptides for drug delivery across membrane barriers. Expert Opin. Drug. Deliv. 5, 105–117
3 Lee, E. J., Jang, E. J., Lee, E., Yu, J., Chung, H. Y. and Jang, Y. J. (2007). Cell-penetrating autoantibody induces caspase-mediated apoptosis through catalytic hydrolysis of DNA. Bioorg. Med. Chem. 15, 2016–2023
4 Suchkov, S.V. (2001). Comparative study of catalytic (DNA-hydrolyzing) and cytotoxic properties of anti-dna autoantibodies. Bull. Exp. Biol. Med. 131, 353–355
5 Kozyr, A. V., Kolesnikov, A. V., Zelenova, N. A., Sashchenko, L.P., Mikhalap, S.V., Bulina, M.E., Ignatova, A.N., Favorov, P.V. and Gabibov, A.G. (2000). Autoantibodies to nuclear antigens: correlation between cytotoxicity and DNA-hydrolyzing activity. Appl. Biochem. Biotechnol. 83, 255–268; discussion 268–259, 297–313
6 Kozyr, A. V., Sashchenko, L. P., Kolesnikov, A. V., Zelenova, N. A., Khaidukov, S. V., Ignatova, A. N., Bobik, T. V., Gabibov, A. G., Alekberova, Z. S., Suchkov, S. V. and Gnuchev, N. V. (2002). Anti-DNA autoantibodies reveal toxicity to tumor cell lines. Immunol. Lett. 80, 41–47
7 Foster, M. H., Kieber-Emmons, T., Ohliger, M. and Madaio, M. P. (1994). Molecular and structural analysis of nuclear localizing anti-DNA lupus antibodies. Immunol. Res. 13, 186–206
8 Ternynck, T., Avrameas, A., Ragimbeau, J., Buttin, G. and Avrameas, S. (1998). Immunochemical, structural and translocating properties of anti-DNA antibodies from (NZBxNZW)F1 mice. J. Autoimmun. 11, 511–521
9 Yanase, K., Smith, R. M., Puccetti, A., Jarett, L. and Madaio, M. P. (1997). Receptor-mediated cellular entry of nuclear localizing anti-DNA antibodies via myosin 1. J. Clin. Invest. 100, 25–31
10 Zack, D. J., Stempniak, M., Wong, A. L., Taylor, C. and Weisbart, R. H. (1996). Mechanisms of cellular penetration and nuclear localization of an anti-double strand DNA autoantibody. J. Immunol. 157, 2082–2088
11 Avrameas, A., Gasmi, L. and Buttin, G. (2001). DNA and heparin alter the internalization process of anti-DNA monoclonal antibodies according to patterns typical of both the charged molecule and the antibody. J. Autoimmun. 16, 383–391
12 Mayor, S. and Pagano, R. E. (2007). Pathways of clathrin-independent endocytosis. Nat. Rev. Mol. Cell. Biol. 8, 603–612
13 Parton, R.G. and Simons, K. (2007). The multiple faces of caveolae. Nat. Rev. Mol. Cell. Biol. 8, 185–194
14 Yanase, K. and Madaio, M. P. (2005). Nuclear localizing anti-DNA antibodies enter cells via caveoli and modulate expression of caveolin and p53. J. Autoimmun. 24, 145–151
15 Reichlin, M. (1998). Cellular dysfunction induced by penetration of autoantibodies into living cells: cellular damage and dysfunction mediated by antibodies to dsDNA and ribosomal P proteins. J. Autoimmun. 11, 557–561
16 Rivadeneyra-Espinoza, L. and Ruiz-Arguelles, A. (2006). Cell-penetrating anti-native DNA antibodies trigger apoptosis through both the neglect and programmed pathways. J. Autoimmun. 26, 52–56
17 Kim, Y. R., Kim, J. S., Lee, S. H., Lee, W. R., Sohn, J. N., Chung, Y. C., Shim, H. K., Lee, S. C., Kwon, M. H. and Kim, Y. S. (2006). Heavy and light chain variable single domains of an anti-DNA binding antibody hydrolyze both double- and single-stranded DNAs without sequence specificity. J. Biol. Chem. 281, 15287–15295
18 Sjogren, B. and Svenningsson, P. (2007). Caveolin-1 affects serotonin binding and cell surface levels of human 5-HT7(a) receptors. FEBS Lett. 581, 5115–5121
19 Arnold, U. and Ulbrich-Hofmann, R. (2006). Natural and engineered ribonucleases as potential cancer therapeutics. Biotechnol. Lett. 28, 1615–1622

20 Hinrichsen, L., Harborth, J., Andrees, L., Weber, K. and Ungewickell, E. J. (2003). Effect of clathrin heavy chain- and alpha-adaptin-specific small inhibitory RNAs on endocytic accessory proteins and receptor trafficking in HeLa cells. J. Biol. Chem. 278, 45160–45170
21 McFarland, M. J., Bardell, T. K., Yates, M. L., Placzek, E. A. and Barker, E. L. (2008). RNA interference-mediated knockdown of dynamin 2 reduces endocannabinoid uptake into neuronal dCAD cells. Mol. Pharmacol. 74, 101–108
22 Thakur, C. S., Xu, Z., Wang, Z., Novince, Z. and Silverman, R. H. (2005). A convenient and sensitive fluorescence resonance energy transfer assay for RNase L and 2',5' oligoadenylates. Methods Mol. Med. 116, 103–113
23 Park, K. J., Lee, S. H., Kim, T. I., Lee, H. W., Lee, C. H., Kim, E. H., Jang, J. Y., Choi, K. S., Kwon, M. H. and Kim, Y. S. (2007). A human scFv antibody against TRAIL receptor 2 induces autophagic cell death in both TRAIL-sensitive and TRAIL-resistant cancer cells. Cancer Res. 67, 7327–7334
24 Mariani, S. M., Matiba, B., Armandola, E. A. and Krammer, P. H. (1997). Interleukin 1 beta-converting enzyme related proteases/caspases are involved in TRAIL-induced apoptosis of myeloma and leukemia cells. J. Cell. Biol. 137, 221–229
25 Duchardt, F., Fotin-Mleczek, M., Schwarz, H., Fischer, R. and Brock, R. (2007). A comprehensive model for the cellular uptake of cationic cell-penetrating peptides. Traffic 8, 848–866
26 Yanase, K., Smith, R.M., Cizman, B., Foster, M. H., Peachey, L. D., Jarett, L. and Madaio, M. P. (1994). A subgroup of murine monoclonal anti-deoxyribonucleic acid antibodies traverse the cytoplasm and enter the nucleus in a time-and temperature- dependent manner. Lab. Invest. 71, 52–60
27 Lajoie, P. and Nabi, I. R. (2007). Regulation of raft-dependent endocytosis. J. Cell. Mol. Med. 11, 644–653
28 Nabi, I. R. and Le, P. U. (2003). Caveolae/raft-dependent endocytosis. J. Cell. Biol. 161, 673–677
29 Botos, E., Klumperman, J., Oorschot, V., Igyarto, B., Magyar, A., Olah, M. and Kiss, A.L. (2008). Caveolin-1 is transported to multivesicular bodies after albumin-induced endocytosis of caveolae in HepG2 cells. J. Cell. Mol. Med. 12, 1632–1639
30 Nichols, B. (2003). Caveosomes and endocytosis of lipid rafts. J. Cell. Sci. 116, 4707–4714
31 Osawa, S., Kajimura, M., Yamamoto, S., Ikuma, M., Mochizuki, C., Iwasaki, H., Hishida, A. and Terakawa, S. (2005). Alteration of intracellular histamine H2 receptor cycling precedes antagonist-induced upregulation. Am. J. Physiol. Gastrointest. Liver Physiol. 289, G880–889.
32 Pelkmans, L., Kartenbeck, J. and Helenius, A. (2001). Caveolar endocytosis of simian virus 40 reveals a new two-step vesicular-transport pathway to the ER. Nat. Cell. Biol. 3, 473–483
33 Andrievskaya, O. A., Buneva, V. N., Baranovskii, A. G., Gal'vita, A. V., Benzo, E. S., Naumov, V. A. and Nevinsky, G.A. (2002). Catalytic diversity of polyclonal RNA-hydrolyzing IgG antibodies from the sera of patients with systemic lupus erythematosus. Immunol. Lett. 81, 191–198
34 Saxena, S. K., Sirdeshmukh, R., Ardelt, W., Mikulski, S. M., Shogen, K. and Youle, R. J. (2002). Entry into cells and selective degradation of tRNAs by a cytotoxic member of the RNase A family. J. Biol. Chem. 277, 15142–15146
35 Pujals, S., Fernandez-Carneado, J., Lopez-Iglesias, C., Kogan, M. J. and Giralt, E. (2006). Mechanistic aspects of CPP-mediated intracellular drug delivery: relevance of CPP self-assembly. Biochim. Biophys. Acta. 1758, 264–279
36 Cheng, F., Mani, K., van den Born, J., Ding, K., Belting, M. and Fransson, L. A. (2002). Nitric oxide-dependent processing of heparan sulfate in recycling S-nitrosylated glypican-1 takes place in caveolin-1-containing endosomes. J. Biol. Chem. 277, 44431–44439
37 De Coupade, C., Fittipaldi, A., Chagnas, V., Michel, M., Carlier, S., Tasciotti, E., Darmon, A., Ravel, D., Kearsey, J., Giacca, M. and Cailler, F. (2005). Novel human-derived cell-penetrating peptides for specific subcellular delivery of therapeutic biomolecules. Biochem. J. 390, 407–418
38 Avrameas, A., Ternynck, T., Gasmi, L. and Buttin, G. (1999). Efficient gene delivery by a peptide derived from a monoclonal anti-DNA antibody. Bioconjug. Chem. 10, 87–93
39 Avrameas, A., Ternynck, T., Nato, F., Buttin, G. and Avrameas, S. (1998). Polyreactive anti-DNA monoclonal antibodies and a derived peptide as vectors for the intracytoplasmic and intranuclear translocation of macromolecules. Proc. Natl. Acad. Sci. USA. 95, 5601–5606
40 Makarov, A. A. and Ilinskaya, O. N. (2003). Cytotoxic ribonucleases: molecular weapons and their targets. FEBS Lett. 540, 15–20